RADIO SPECTRUM OF TWO ACTIVE REGIONS

(Results of the Total Solar Eclipse of Nov. 12, 1966)

by

Franca Chiuderi Drago†

Institute for Space Studies
Goddard Space Flight Center, NASA
New York, New York

MARY

The results of the total solar eclipse of November 12,1966, observed at 8 different wavelengths between 3 and 21 cm., are studied and the spectrum of two active regions present on the disk is deduced. The shape of the more intense source spectrum presents a maximum at $\lambda \sim 10$ cm indicating, at first sight, the non-thermal origin of the emission; it is then shown that the observed flux increase with the wavelength is completely due to geometrical effects. From the Laplace transform of the brightness temperature of this source, the following quantities are deduced:

a) the mean and central temperature of the coronal condensation.

b) the $\int_{\text{corona}} N^2 dh$ (N = electron density). Both these quantities are in good agreement with optical observations.

† On leave from Osservatorio Astrofisico di Arcetri-Firenze (Italy)

(1) Introduction

The total solar eclipse of November 12, 1966 was observed in South America by several groups of radio astronomers. Our research has been made possible through the cooperation of some observers who provided us with copies of their eclipse records obtained at several different wavelengths (w.l.'s). The names of these observers as well as the observed w.l.'s and all the characteristics of the eclipse are summarized in table I.

It is well known that the study of eclipse records can give much important information on the structure of the active regions and on the brightness distribution of the solar disk in all cases where the conventional instruments do not have enough resolving power to distinguish the different points of the solar surface: this fact usually happens with radio or X-ray observations. By using the results of the eclipse of May 20, 1966, for instance, many interesting results on the structure of active regions were deduced both from X-rays (Landini et al., 1969; Simon, 1969) and radio observations (Drago and Noci, 1969). With regard to the latter, a very high resolving power was obtained in six different directions by observing the eclipse from three different places.

In this case the angle between the two directions of occultation, as seen from Ancon and Bagè, is only $\simeq 3^{\circ}$, (see Table I) so that none of the information obtained on May 20 on the shape and brightness distribution of the sources can be derived.

In the present research, the peculiar feature is given by the complete spectrum between 3 and 21 cm where all the observations

TABLE I

Observers	Locality	Optical Contacts I	II	III	IV	Path angle α	Obs. λ	Remarks
J. Castelli R. Straka A.F.C.R.L. Cambridge (Mass) U.S.A.	Ancon (Peru) -11°47' + 77°04'	U.T. h m s 11 58 00	U.T. h m s 13 02 02	U.T. h m s 13 03 07	U. T. h m s 14 15 12	≈10°30'	(cm) 3.4 6.0 11.1 21.2	
P. Kaufmann Mackenzie Observ. S. Paolo, Brasil	Bagè (Brasil) -31°22' + 54°06'	12 45 47	14 04 07	14 06 05	15 31 30	≈13°30'	4.3	Also polarization measurements
G. Tofani Oss.Astr.Arcetri Firenze, Italy	Bagè (Brasil) -31°22' + 54°06'	12 45 47	14 04 07	14 06 05	15 31 30	≈13°30'	3.1 6.7 9.1	The 6.7 cm record is available only from ≈ 13^h30^m U.T.

are made with the same resolving power. Many inconsistencies may in fact arise when observations with instruments of different resolving power are compared, this is in fact equivalent to comparing information from different parts of the source.

(2) Localization and Identification of the Sources

The best way to localize the active regions on the solar disk is to consider the derivative of the occultation curve $\dot{\Phi}(t)$ instead of the occultation curves themselves.

In fact, when a region brighter than the background is covered by the moon at a given time t, a corresponding change in the slope of the occultation curve is noticed: therefore, if we plot the behavior of the slope (the derivative) of the occultation curve vs. time, the presence of a source is immediately apparent.

In Figures 1a and 1b, the $\dot{\Phi}(t)$ curves observed in Ancon and Bagè, respectively, are shown. $\dot{\Phi}(t)$ is the difference between two consecutive values of Φ: $\dot{\Phi}(t) = \Phi(t + \Delta t) - \Phi(t); \Delta t = 1$ minute.

The presence of a very strong source (A), situated near the center of the disk, and another less intense source (B), located in the western hemisphere, is evident.

The localization on the solar disk of these two sources is shown in Figure 2. The corresponding optical plages are respectively:

(A) McMath No. 8575 (13N-15E)

(B) McMath No. 8572 (18N-29W)

Also many other peaks in the $\dot{\Phi}(t)$ curves were identified as small radio sources correlated with some filaments or prominences,

but in this paper we will consider only the two strongest sources, A and B.

In both sets of $\dot{\Phi}(t)$ curves, the source (A) presents the same characteristic: it is double when it is covered and single when it is uncovered; the two minima in the covering phase correspond to the occultation of two spots (following the Fraunhofer map) and the geometry of the eclipse was such that they were uncovered together (see Figure 2). The separation between the two components of the double source in the E-W direction ranges from 0'.75 to 1' depending on the w.l.

A more careful examination of the $\dot{\Phi}$ curves shows that source A, after the two strong minima, presents a smoother tail: the first (double) part of the source will be called in the following: (A1), the second one (A2).

(3) Dimensions, Emitted Flux and Equivalent Temperature

The dimensions of the sources in the advancing moon's limb direction and the relative emitted flux at each w.l. can be easily deduced from the $\dot{\Phi}$ curves. In fact, calling t_1 and t_2 the beginning and the end of the occultation of a source s in the covering (c) phase and t'_1 and t'_2 the analogous times in the uncovering (u) phase, (t_1,t_2 and t'_1, t'_2 depends on λ) the dimensions d_c and d_u in the two directions are given by:

$$d_c = v_c(t_2-t_1)$$

$$d_u = v_u(t'_2-t'_1)$$

where v_c and v_u are the speeds of the advancing moon's limb.

$$v_c = 3.13\ 10^{-2}\ \frac{R_\odot}{min},\ V_u\ 2.77\ 10^{-2}\ \frac{R_\odot}{min}\quad \text{(Ancon)}$$

$$v_c = 2.55.10^{-2}\ \frac{R_\odot}{min},\ v_u = 2.34\ 10^{-2}\ \frac{R_\odot}{min}\ \text{(Bagè)}$$

The relative emitted flux can also be derived from the $\dot{\Phi}$ curves making some hypotheses on the quiet sun radiation. The flux Φ_s emitted by a source s is given, in fact, by the integral

$$\Phi_s(c) = \int_{t_1}^{t_2} \dot{\Phi}_s(t)\,dt = \int_{t_1}^{t_2} \left[\dot{\Phi}(t) - \dot{\Phi}_q(t)\right] dt$$

$$\Phi_s(u) = \int_{t_1'}^{t_2'} \dot{\Phi}_s(t)\,dt = \int_{t_1'}^{t_2'} \left[\dot{\Phi}(t) - \dot{\Phi}_q(t)\right] dt$$

the quantity $\dot{\Phi}_q(t)$ indicates the derivative of the flux coming only from the quiet disk without sources

$$\Phi_q = \Phi_\odot - \sum_1^N{}_i\ \Phi_{si}$$

where $\Phi_\odot$ is the total observed flux and N is the number of sources. The behavior of the $\dot{\Phi}_q$ curves can be easily computed by the occultation of a uniformly bright disk, the constant (unknown) brightness of the quiet Sun can be deduced by imposing on these curves to fit the observed $\dot{\Phi}$ curves in the times intervals where no sources are occultated. We have in fact:

$$\dot{\Phi}(t) = \dot{\Phi}_q(t) + \dot{\Phi}_{si}(t) \qquad t_1(si) < t < t_2(si)$$
$$t'_1(si) < t < t'_2(si)$$

and

$$\dot{\Phi}(t) = \dot{\Phi}_q(t)$$

when no sources are involved. The ratio between Φ_s and the total solar flux measured in the same relative units gives the relative flux of the source. To derive absolute values of the flux, we used a solar spectrum derived from all the radio observations published in the Quarterly Bulletin (see Figure 3).

From the above computed diameters d_c and d_u we can derive, assuming circular symmetry, the emitting surface of the source: $\frac{S_{si}}{S_\odot} = \frac{1}{4}\left(\frac{d_i}{R_\odot}\right)^2$. The scattering between (c) and (u) results may give an idea of the validity of this assumption. The obtained fluxes and surfaces are shown in Figure 4. From these quantities we can compute the equivalent temperature of the source given by:

$$\therefore \quad T_e = \frac{\lambda^2}{2k\Omega_\odot} \frac{\Phi_s}{S/S_\odot}$$

where $\Omega_\odot$ is the solid angle of the whole Sun. The term $T_q = \frac{\lambda^2 \Phi_q}{2k\Omega_\odot}$ must be added in order to find, for $\Phi_s \to 0$, the correct value $T_e = T_q$ instead of $T_e = 0$. The equivalent temperature, averaged on (c) and (u) measurements are shown in table II. The reason why in table II only (c) measurements are given for A2 at $\lambda > 6$cm,

will be discussed below. In order to decrease the scattering, we have used the mean curves obtained with a polinomial fit, (shown in Figure 4) instead of the single values of $S(\lambda)/S_{\odot}$. The values used for $\Phi_s(\lambda)$ on the contrary, are those derived from the observations.

TABLE II

λ / Source	3.1	3.4	4.3	6.0	6.7	9.1	11.1	21.2
A1	174±3	262±7	349±5	601±25	748 (*)	1038±64	1330±30	1670±93
A2	66±9	84±2	109±2	199±17	251 (**)	445 (**)	444 (**)	857 (**)
B	39±0	47±6	62±3	101±5	— (*)	212±7	362±1	947±78

(*) At = 6.7 cm source B is not detectable and source A1 is measurable only in (u)-phase.

(**) Only (c)-measurements

The equivalent temperatures so determined for the three sources do not refer to the same portion of the solar disk because the $S/S_{\odot}$ is in general a function of λ.

This problem concerning source A, which we consider to be the most interesting one, will be discussed in detail in paragraph (5).

If we consider carefully the different behavior of $\Phi(A1)$, $\Phi(A2)$ and $\frac{S}{S_{\odot}}(A1)$, $\frac{S}{S_{\odot}}(A2)$ in (c) and (u) phase we must conclude that the dimensions of source A2, as those of all the other ones,

increase with the w.l. but for $\lambda \gtrsim 6$ cm, the source seems to shift its mean position toward the solar limb in such a way that part of it becomes uncovered together with A1: the flux attributed to A1 is in fact always larger in the (u) phase than in the (c) phase, while the surface of A2 behaves in the opposite way. (A schematization of source A is shown in Figure 5.) Shown in the upper left side curve of Figure 4 is the total flux emitted by the entire source A,

$$\Phi(1+2) = \Phi(A1) + \Phi(A2)$$

averaged on the (c) and (u) phase results; we see that the discrepancies between (c) and (u) are really negligible when the entire source is involved, supporting our previous hypothesis on the structure of source A.

(4) Polarization Measurements

The only polarization measurements on the eclipse records are those at $\lambda = 4.3$ cm. According to this record, only two appreciable changes of polarization are present during the eclipse, both correlated with the occultation of source A: a decrease of left-handed polarization in (c) phase began at t = 1329 U.T., the same time of the second minimum of $\dot{\Phi}(A1)$; an increase of the same amount in the (u) phase began at 1451 U.T., at the time corresponding at the maximum of $\dot{\Phi}(A1)$ (see Figure 1B). We can therefore conclude that the only polarized source was source A and, inside this one, no polarized flux comes from the region above the first covered spot. From the time interval in which $\frac{dP}{dt} \neq 0$ we may also derive the dimensions of the polarized region at 4.3 cm which turns out to be

1'.7 (c-direction) and 1'.2 (u-direction). (In our schematization this polarized region also covers part of A2.) More details on the behavior of $\frac{dP}{dt}$ at 4.3 cm are given by Kaufmann (1968). If we assume also that at other w.l.'s as at 4.3 cm, all the observed polarized radiation comes from the source A, we can derive the polarization percentage of the source, P_s, from polarization measurements of the total solar flux, $P_\odot$:

$$1) \qquad P_s = P_\odot \times \frac{\Phi_\odot}{\Phi_s}$$

Data referring to the total solar polarization $P_\odot$(%) and the obtained results for the source P_s(%) are summarized in table III.

TABLE III

λ (cm)	3.2	4.3	8	15	30
$P_\odot$(%)	1.89L(*)	2.3L(**)	2.06L(*)	0.55L(*)	0.31L(*)
P_s(%)	21.6L	19.7L	10.5L	2.0L	1.5L(?)

(*) Courtesy of Dr. Tanaka

(**) From Kaufmann et al. (1967)

The last value of the source polarization percentage is uncertain because the w.l. λ = 30 cm is out of our range of observation, and therefore the value of Φ_s was extrapolated in order to compute P_s from formula (1).

The percentage of polarization is rather small for a Slowly Varying (S) Component source, but we must remember that only part of source A was polarized, while the values of P_s in Table III are in percentage of the total flux emitted by A. But as we do not know the size of polarized regions at all the w.l.'s, we cannot perform further computation.

(5) The Sources Spectrum

The spectra of A2 and B are slightly decreasing with the w.l. which seems to indicate a complete thermal origin of the radiation. The reason for the scattering of Φ(A2) and $\frac{S}{S_\odot}$ (A2) has already been discussed in paragraph (3). With regard to the source B we see that the agreement between Φ(c) and Φ(u) is quite good, while the scattering on the surfaces is considerable. This may indicate absence of circular symmetry, but we must remember that the computed surface is proportional to d^2 so that the relative errors on the surfaces are twice those on d (this is the reason that we preferred to use the mean curves instead of the single values). Contrary to those just now discussed the spectrum of A1 presents the characteristic shape of the S-Component spectrum with a sharp maximum at $\lambda \sim 10$ cm and decreases both toward longer and shorter w.l.'s.

The spectrum of the S-Component is usually derived by subtracting the quiet Sun spectrum from the total solar spectrum when some active region is present; in this way no information about the emitting surface is available and it is usually assumed constant when deriving the equivalent temperature.

The flux increase vs. λ of the S-Component in the range 3-10 cm is usually interpreted as a proof that the emission cannot be completely of thermal origin.

We will now show that in this case the increase of the flux with the w.l. is due to the rise of the emitting surface rather than a real increase in the brightness of the source.

To show this, we must consider only the flux $\phi_{\odot}(\lambda)$ coming from a fixed portion of the source $\bar{S}$ common to all the observed w.l.'s; let us consider in both sets of records two fixed points, $\bar{t}_1$ and $\bar{t}_2$ at all w.l.'s. (We used for this computation only the (c) phase measurements, otherwise, as already mentioned, a part of A2 would also be involved.) The points, $\bar{t}_1$ and $\bar{t}_2$ were those corresponding to the beginning and to the end of occultation of the whole source A1 at λ = 3.4 and 6.0 cm (Ancon $\bar{t}_1$ = 1230, $\bar{t}_2$ = 1235 U.T.) and λ = 4.3 cm (Bagè $\bar{t}_1$ = 1325, $\bar{t}_2$ = 1331 U.T.). As the position of the moon as seen from Ancon and Bagè at the above instants were practically coincident, these two points determine on the solar surface the same strip of thickness $\bar{d} = v_c^* (\bar{t}_2 - \bar{t}_1) \approx 0.155\ R_{\odot}$. Therefore, in the assumed circular symmetry, the considered fixed portion of the source at all the w.l.'s will be:

$$\bar{S} = \frac{\bar{d}^2}{4} \approx 0.6 \times 10^{-2} S_{\odot}$$

Let us now consider at all the w.l.'s only the flux given by the integration of $\dot{\phi}_s$ between $\bar{t}_1$ and $\bar{t}_2$.

$$\Phi_{12} = \int_{\bar{t}_1}^{\bar{t}_2} \dot{\Phi}_s(t)\, dt$$

For the w.l.'s λ = 3.4, 4.3 and 6.0 cm. We have

$$\frac{\bar{S}}{S_\odot} = \frac{S}{S_\odot} \approx 0.6 \cdot 10^{-2}$$

$$\Phi_0 = \Phi_S = \Phi_{12}$$

where $\frac{S}{S_\odot}$ is the total surface of A_1 given in Figure 4. For λ = 3.1 and $\lambda > 6$ cm, we have $S > \bar{S}$; assuming in $S - \bar{S}$ a uniform mean brightness distribution B, we can easily deduce the flux emitted by the portion $\bar{S}$ of the source, from the solution of the system:

2)
$$\Phi_S = B_0 \bar{S} + B(S - \bar{S})$$

$$\Phi_{12} = B_0 \bar{S} + B S_1$$

Where B_0 is the mean brightness of $\bar{S}$ ($B_0 \bar{S} = \Phi_0$) and S_1 is the portion of the ring $S - \bar{S}$ covered between the times $\bar{t}_1$ and $\bar{t}_2$ (Figure 6). The values thus obtained of Φ_0 are shown in Figure 7. We see that the behavior is completely changed with respect to the previous spectrum of A_1: no more increase of the flux with the w.l. is noticed. An analogous measurement would be difficult to make out of eclipses: in fact, if the spectrum is built by comparing results coming from different high resolving power instruments, each of them will give the flux averaged on a surface which is, at minimum, as large as the antenna lobes which are not always equal to each other. Therefore, it would be impossible in this case to measure, over the entire spectrum, only the flux coming from a fixed portion of the

source (unless the source at all w.l.'s is larger than the largest antenna lobe). From Figure 7 we can, therefore, conclude that the sharp maximum observed in Figure 4 is due to an increase of the emitting surface and does not support the non-thermal origin of the radiation.

We think that this is a rather important result even if it is derived only in one particular case: the increase of the emitting surface with the w.l. is in fact quite common in the radio active regions (Newkirk, 1961; Tlamicha, 1968). From the values of Φ_o we can now compute the equivalent temperature of the central part of the source $\bar{S}$:

$$T_{\bar{S}} = \bar{c}\ \lambda^2 \Phi_o + T_q$$

with $\bar{c} = \frac{1}{2k\Omega_\odot} \cdot \frac{1}{\bar{S}/S_\odot}$

This equivalent temperature represents the central brightness temperature of the source averaged on the surface $\bar{S}$. (It gives about the same brightness temperature which would be measured with an antenna beam of $\simeq 2'$). The upper and lower limits of this mean brightness temperature can be evaluated assuming respectively:

a) B = 0 out of $\bar{S}$: $T_{max} = \bar{c}\ \lambda^2 \Phi_{12} + T_q$

b) Uniform brightness on the area $\bar{S} + S_1$: $T_{min} = \bar{c}\ \lambda^2 \Phi_{12} \frac{\bar{S}}{\bar{S}+S_1} + T_q$

We said in paragraph (2) that the source A_1 presents a double structure: the two minima corresponding to the occultation of the

two spots are both inside surface $\bar{S}$. In these radio spots the brightness temperature certainly reaches higher values than $T_{\bar{S}}$. However, a computation of the brightness temperature inside the radio spots would be meaningless because of the large errors involved: If we carefully consider the $\dot{\Phi}$ behavior in Figure 1a) and 1b) we see in fact that the position of the maximum between the two minima of A_1 varies within one minute depending on the w.l. As the occultation of each radio spot lasts for about 2, 3 minutes only, this variation would affect the results with 30%, 50% errors.

6) Discussion

The computed equivalent temperature for the whole A_1 source (T_S) and for its central region $\bar{S}$ ($T_{\bar{S}}$) are plotted in Figure 8: the broken line gives $T_b = k\lambda^2$ which represents the steepest acceptable slope within the thermal emission hypothesis: we see that the fit of the observed temperature (full line) presents a slope always lower than λ^2 supporting the thermal origin of the radiation in both sets of temperature. The fit is made in fact with the function

$$T(\lambda) = T_1 \left(1 - e^{-\alpha\lambda^2}\right) + T_o \qquad 3)$$

which has always $\frac{d}{d\lambda}\left(\frac{T(\lambda)}{\lambda^2}\right) \leq 0$

The value of T_o was imposed a priori $T_o = 10^4$ °K, while the parameter T_1 and α were deduced with an iterative least square method (the parameter α is not linearly contained). The results are the

following:

T_s	$T_{\bar{s}}$
$T_1 = 1.675 \times 10^6$ °K	$T_1 = 2.288 \times 10^6$ °K
$\alpha = 1.215 \times 10^{-2}$ cm^{-2}	$\alpha = 0.960 \times 10^{-2}$ cm^{-2}

The quantity $T_c = T_1 + T_o = \lim_{\lambda \to \infty} T(\lambda)$ can be considered as an estimation of the coronal temperature above the active regions. We see that there are no big differences between the coronal temperature deduced from the two sets of data indicating the almost constant temperature going from the center to the peripheral region of the coronal condensation. The obtained values of the temperature $T_c = 1.7 \times 10^6$ °K and $T_c = 2.3 \times 10^6$ °K are both very plausible for a coronal condensation.

If we neglect the effect of the magnetic field, a rough evaluation of the electron density in the coronal condensation can also be obtained in the following way. This hypothesis is supported by the fact that the polarized area is less than 1/3 of $\bar{S}$ (following 4.3 cm Bagè observations), and the polarization percentage is generally low. Let us apply to the observed $T_{\bar{s}}$ the method used by Piddington (1954), Moriyama (1961) and Drago and Noci (1969) in order to determine a relationship between the electron density N and the temperature T in the solar atmosphere from the Laplace transform of the brightness temperature. Let us consider the following form of the integral of the transfer equation, obtained from the exact one having assumed the refraction index n = 1, (which is true with a very good approximation up to $\lambda \leq 50$ cm):

$$\frac{T_b(x)}{x} = \int_0^\infty T(\sigma)\, e^{-\sigma x}\, d\sigma$$

where T_b is the brightness temperature, $x = \frac{\lambda^2}{c^2} = \frac{1}{\nu^2}$ and $d\sigma = -\frac{\xi N^2 dh}{3/2 \cos\theta}$. ($\xi$ is a slowly varying term which assumes the value $\xi = 0.11$ in chromosphere and $\xi = 0.16$ in corona with h (cm) $N(cm^{-3})$; θ is the angle between the solar radius and the line of sight: for the source A_1 $\theta \simeq 13^o$). We see that the function $\frac{T_{b(x)}}{x} = \frac{c^2}{\lambda^2} T_b(\lambda)$ is formally the Laplace transform of $T(\sigma)$ and therefore

$$T(\sigma) = \mathcal{L}^{-1}\left[\frac{T_b(x)}{x}\right]$$

where $\mathcal{L}^{-1}$ indicate the inverse Laplace transform. If we identify the brightness temperature of the central region of the source with T_s given by formula 3, we obtain

$$T(\sigma) = T_1 + T_o = T_c \qquad \sigma < \sigma_o = c^2\alpha = 8.64 \times 10^{1}$$

$$T(\sigma) = T_o \qquad \sigma > \sigma_o$$

The good fit of the observed temperature with the function given in formula 3, indicates that assuming also a very simplified model of temperature with an abrupt jump from chromospheric to coronal values, we can satisfactorily account for the observed spectrum.

From σ_0 and T_c we can determine the quantity

$$\int_{h_0}^{\infty} \xi N^2 dh = T_c^{3/2} \sigma_0 \cos\vartheta$$

where h_0 is the height above the photosphere where the temperature jump takes place. Assuming $\xi = 0.16$ we find

$$4) \qquad \int_{h_0}^{\infty} N^2 dh = 1.83 \cdot 10^{29} \ cm^{-5}$$

The same integral performed with the central electron densities of the coronal condensation observed by Waldmeyer (1963) gives:

$$\int_{.02\,R_\odot}^{.30\,R_\odot} N^2 dh = 1.11 \cdot 10^{29} \ cm^{-5}$$

As the part of the corona at $h > 0.3\ R_\odot$ cannot account for the quantity $0.7.10^{29}$ cm^{-5} which is missing, this discrepancy can be due either to the fact that we are dealing with a coronal condensation denser by a factor ~ 1.3 than the Waldmeyer one, or, more probably, it may be a consequence of the assumed schemetization. The level h_0 in our schemetization would probably be a good approximation of the flexus point in a more realistic model of T(h): identifying it with the basis of the corona it means to overestimate integral 4). As already mentioned, this is a too simplified schemetization of the solar atmosphere to be considered a "model"; however, the acceptable values of T_c and $\int_{\text{corona}} N^2 dh$, besides the very

good approximation of the observed brightness temperature with the exponential function (formula 3) mean, in our opinion, that our observations support an extremely steep gradient of temperature in the transition layer between chromosphere and corona. This result is opposite to the one found with the same method by Piddington (1954) who required a very mild temperature gradient to explain the radio spectrum of the quiet Sun. However, we want to point out that the model obtained with the Laplace transform method depends very much on the chosen function to interpolate the observed data. Piddington used a 2nd degree polinomial in λ which, in the range of frequencies we considered, gives a very good fit for the quiet Sun, but a very bad one for our spectrum, moreover, it diverges for $\lambda \to \infty$ giving a coronal temperature also tending to infinite, which cannot be acceptable. A very steep gradient of temperature in the transition layer is instead a necessary characteristic, in the quiet Sun atmosphere, in order to explain the observed U.V. solar spectrum (Athay 1966; Zirin 1969).

As the transition layer is a very unknown region of the solar atmosphere, we think that a confirmation of the U.V. results in the radio w.l. range would be very interesting. A more accurate analysis of this spectrum as well as of the quiet Sun radio spectrum is now in progress in order to derive, with the above method of the Laplace transform, a model of the solar atmosphere both for the quiet atmosphere and for active regions.

ACKNOWLEDGMENTS

This research has been made possible through the courtesy of J. Castelli, P. Kaufmann, R. Straka and G. Tofani to whom I wish to express my best thanks. Thanks are also due to Dr. A. Skumanich and especially to Prof. G. Noci for many helpful discussions and suggestions.

The author is holding a fellowship from the European Space Research Organization (E. S. R. O.) and wishes to thank Dr. Robert Jastrow for the hospitality extended to her at the Goddard Institute for Space Studies.

REFERENCES

Athay, R. G.: 1966, Astrophys. J. 145, 3, 784

Drago, F. G. and Noci, G.C.: 1968, Solar Phys. 7, 276

Kaufmann, P.: 1968, Solar Phys. 4, 58

Kaufmann, P., Matsura, O.T. and Marques dos Santos, P.: 1967, Icarus 7, 380

Landini, M., Noci, G., Russo, D. and Tagliaferri, G.L. Presented at XII Cospar Meeting, Prague, May, 1969.

Moriyama, F.: 1961, Tokyo Astron. Obs. Ann. 7, 127

Newkirk, G.: 1961, Astrophys. J. 133, 983

Piddington, J.H.: 1954, Astrophys. J. 119, 531

Simon, G.: 1969, Solar Phys. 7, 295

Tlamicha, A.: 1968, Solar Phys. 5, 377

Waldmeier, M.: 1963, Z. f. Astrophys. 56, 291

Zirin, H.: 1969, Solar Phys. 9, 77

FIGURE CAPTIONS

Figure 1a: Slope of the occultation curves observed in Ancon.

1b: Slope of the occultation curves observed in Bagè.

Figure 2: Localization of the radio sources on the Fraunhofer Map of November 12, 1966. The times corresponding at the positions of the moon are from Ancon.

Figure 3: Spectrum of the total solar flux observed on November 12, 1966, used as a calibration spectrum of the sources

Figure 4: Left side: Spectrum of the observed sources in absolute units ($J = 10^{-22}$ watt/m^2 Hz) Right side: Behavior of the observed sources area vs λ in hundredth of solar surface. In source A the outside scale is referred to part 1, the inside scale to part 2.

Figure 5: Schemetization of the structure of source A: full line represents the source contour at $3.cm \leq \lambda \leq 6.cm.$, while dotted line indicates the source contour at a generical wavelength $\lambda > 6.cm.$ (In figs. 5 and 6 moon's and source radii are not in scale)

Figure 6: Schemetization of the source used to compute the central equivalent temperature $T_{\bar{s}}$: full line indicates the contour of $\bar{s}$, dotted line the one of the whole source Al; shaded area represents the surface S_1 in Eq. (2).

Figure 7: Spectrum of the flux Φ_o emitted by the surface $\bar{s}$. The curve is a second degree polinomial fit.

Figure 8: Spectrum of the equivalent temperatures T_s and $T_{\bar{s}}$: broken line gives $T \sim \lambda^2$; full line the best fit made with formula (3). The three bars in the right diagram indicate T_{min} and T_{max} as computed in paragraph 5.

TABLES

Table I: Summary of all parameters of observation. α is the angle formed by the mean direction of the velocity of the moon's center and the solar equator, measured from west to north in a reference frame having its origin in the center of the solar disk.

Table II: Equivalent temperature of the sources (unit: 10^{3o}K). The errors indicate discrepancies between covering and uncovering measurements.

Table III: Polarization measurements in percentage of the total solar flux, $P_{\odot}$(%) and of the flux emitted by source A, P_s(%).

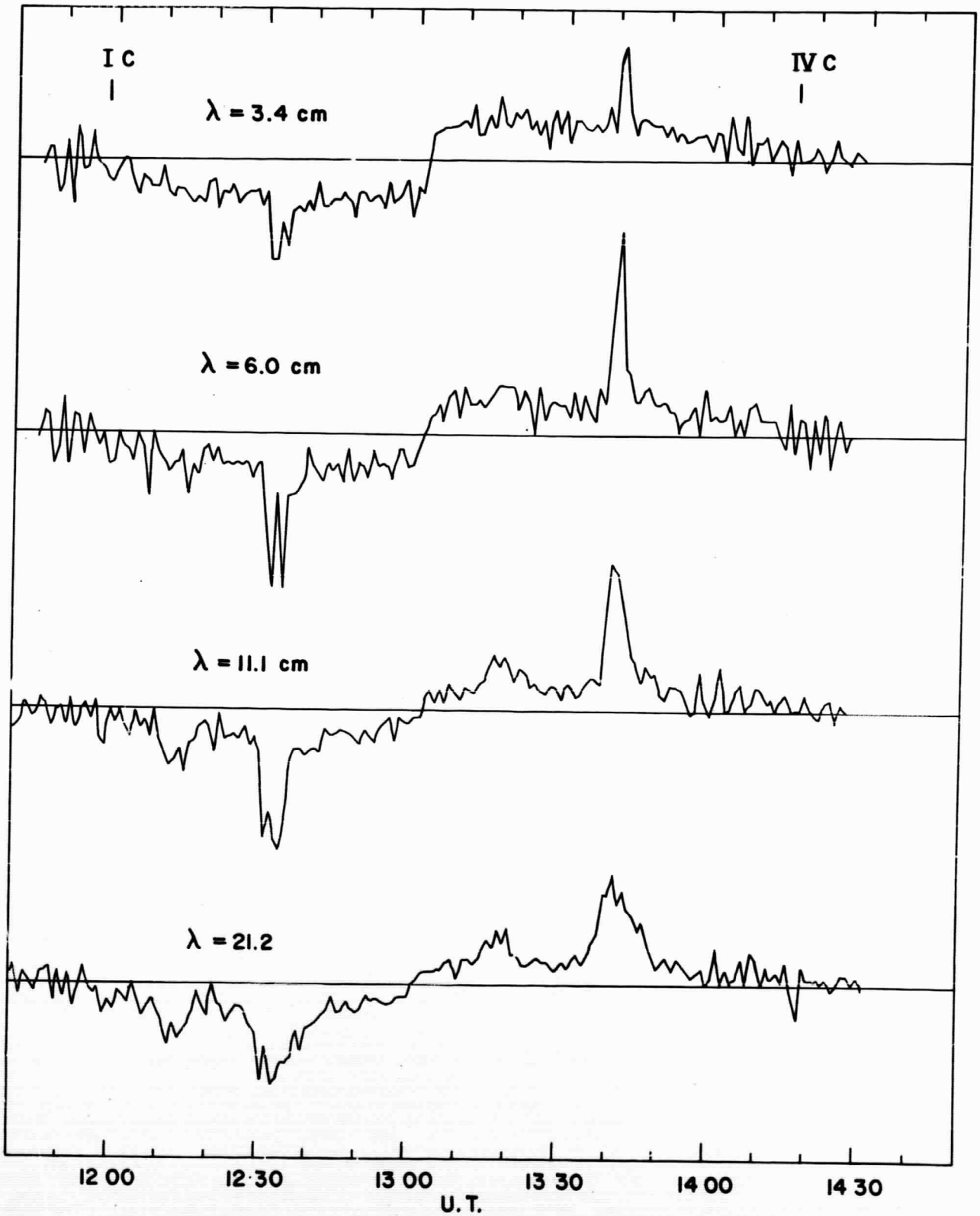
I C
IV C
λ = 3.4 cm
λ = 6.0 cm
λ = 11.1 cm
λ = 21.2
12 00
12 30
13 00
13 30
14 00
14 30
U.T.

Fig. 1a

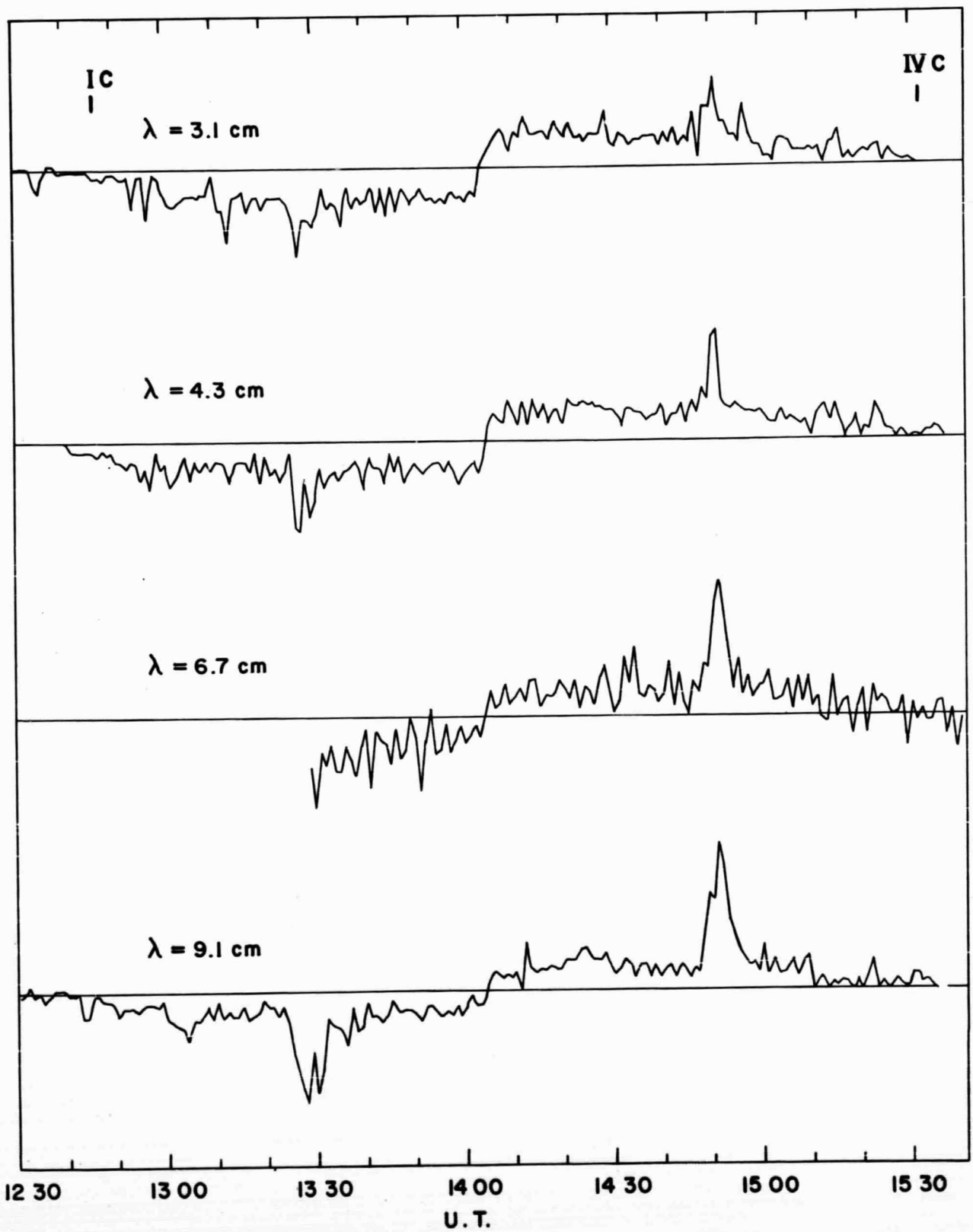
I C
IV C
λ = 3.1 cm
λ = 4.3 cm
λ = 6.7 cm
λ = 9.1 cm
12 30
13 00
13 30
14 00
14 30
15 00
15 30
U. T.

Fig. 1b

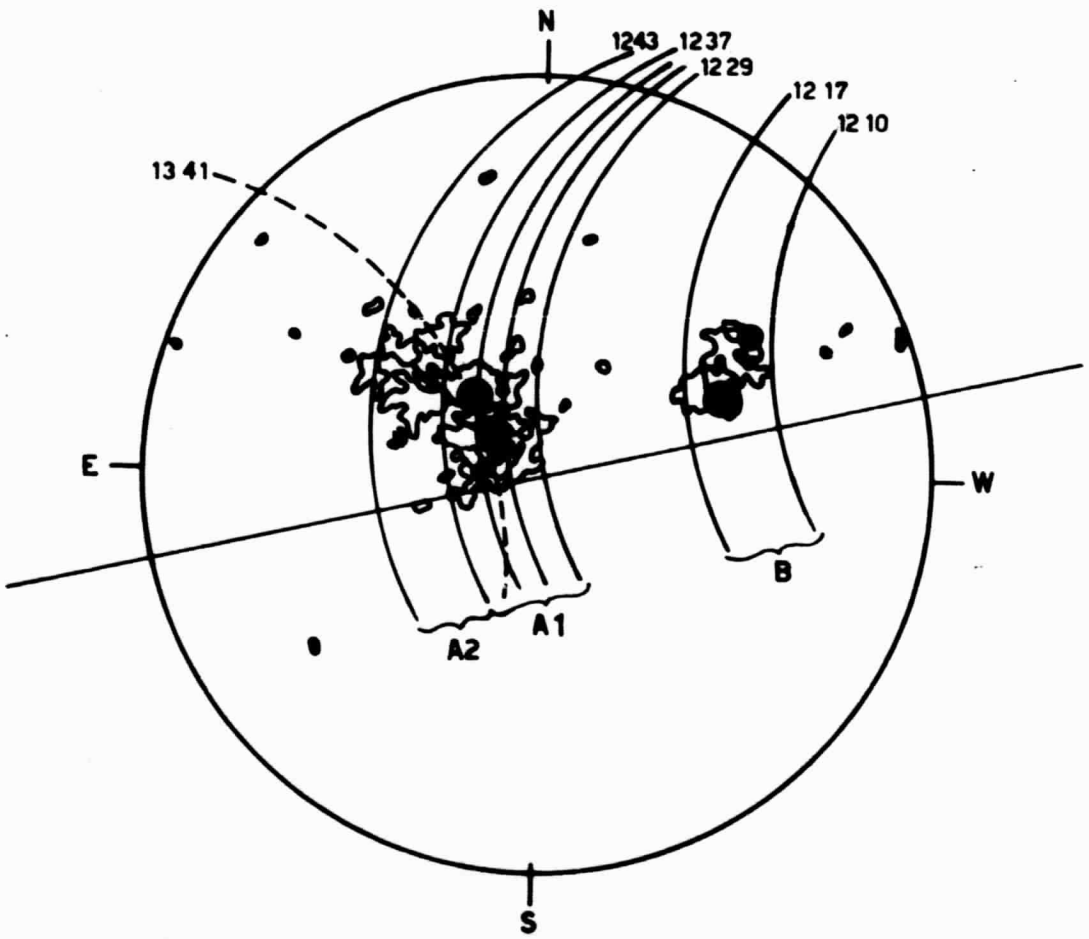

Figure 2)

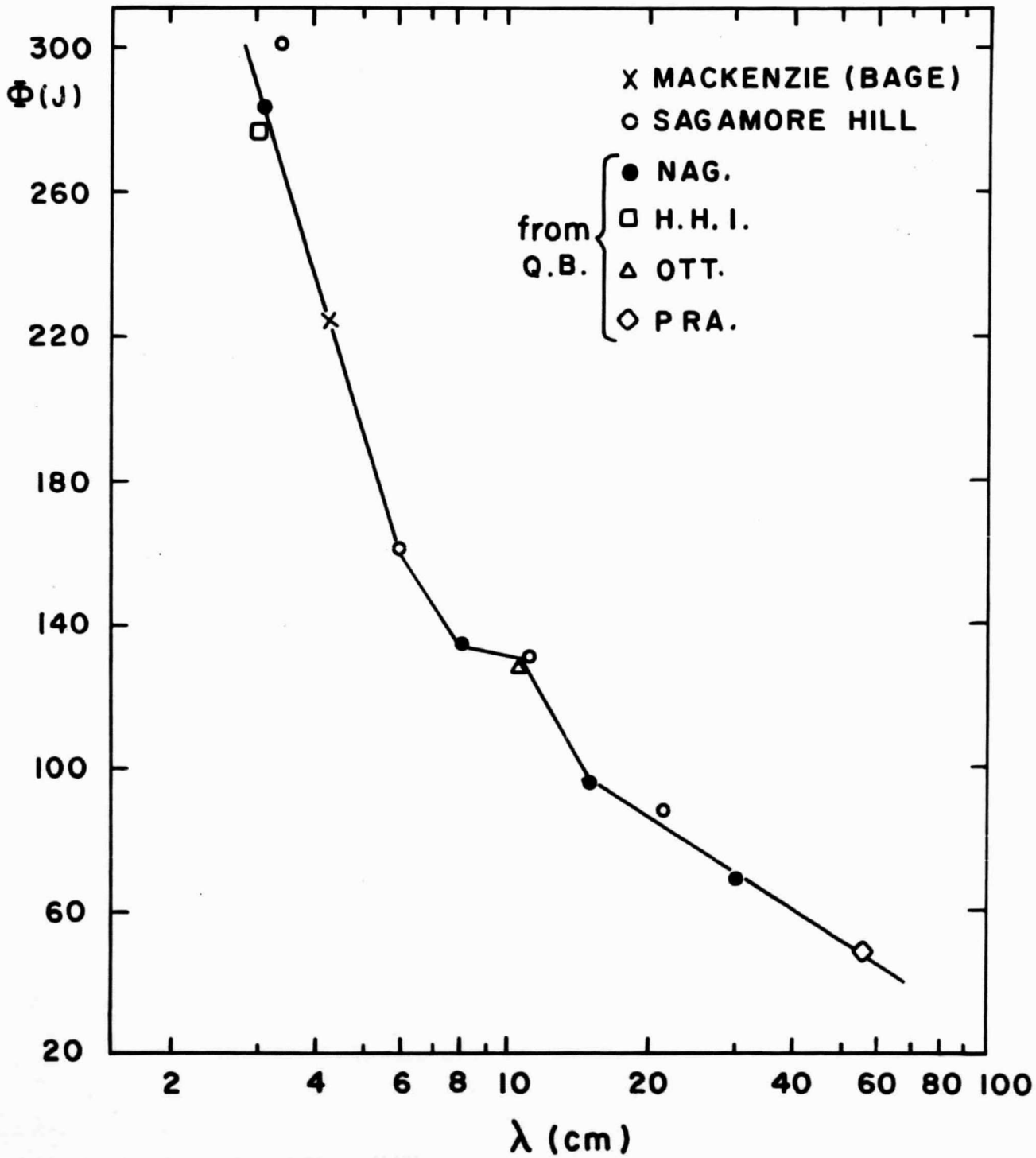
300
Φ(J)
260
220
180
140
100
60
20
2
4
6
8
10
20
40
60
80
100
λ (cm)
X MACKENZIE (BAGE)
o SAGAMORE HILL
from Q.B.
● NAG.
□ H.H.I.
△ OTT.
◇ PRA.

Fig. 3

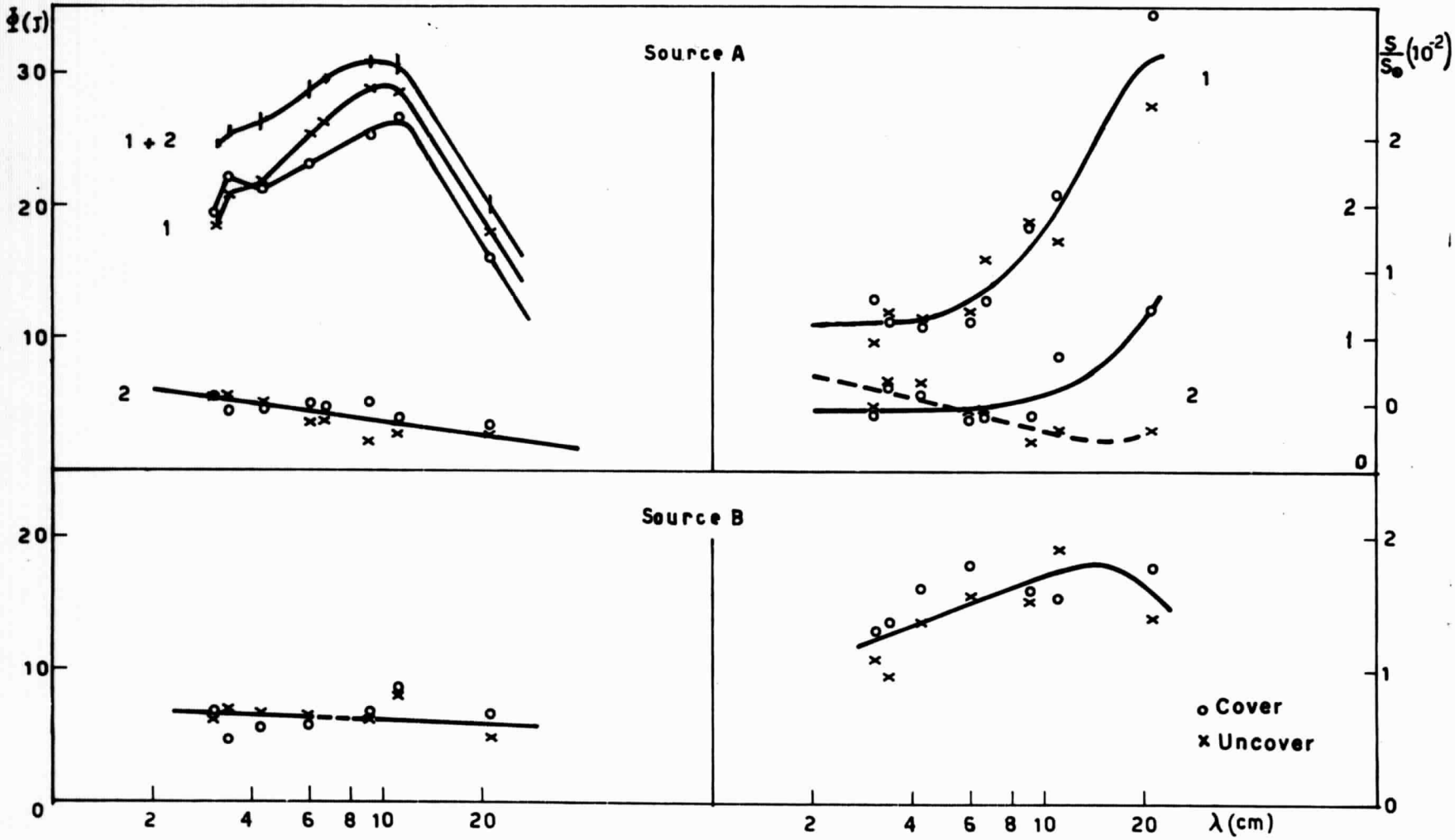

Fig. 4

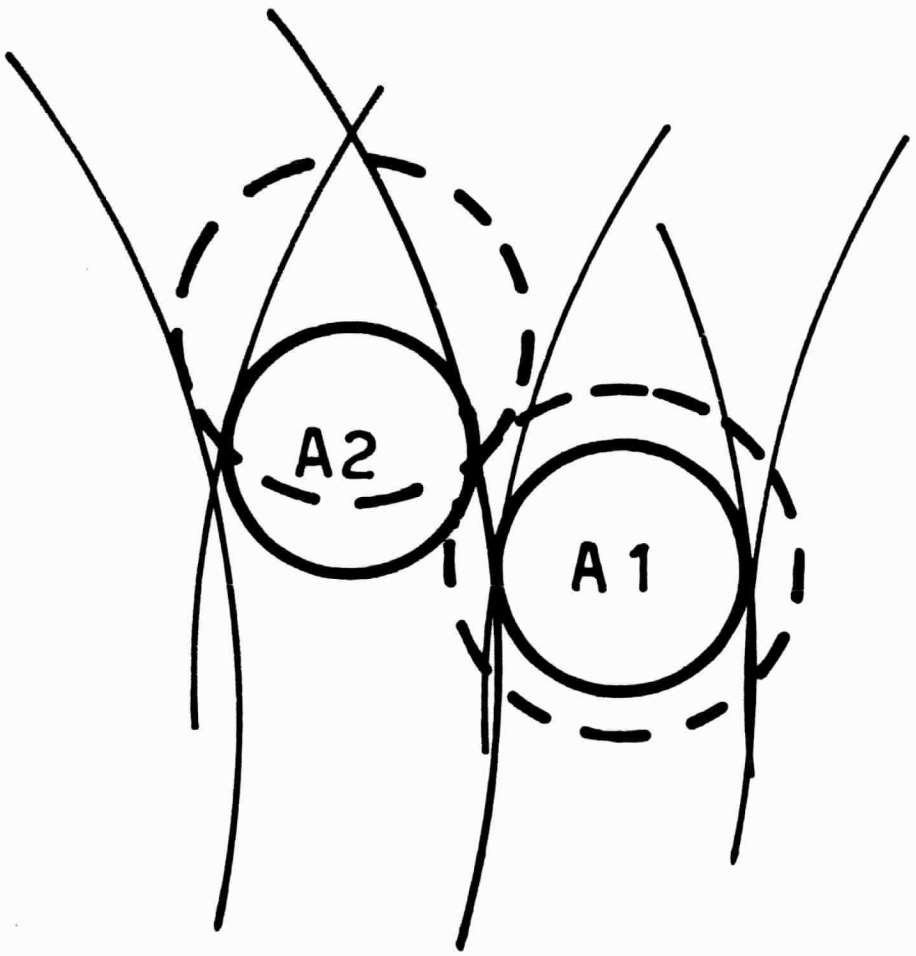

Fig. 5

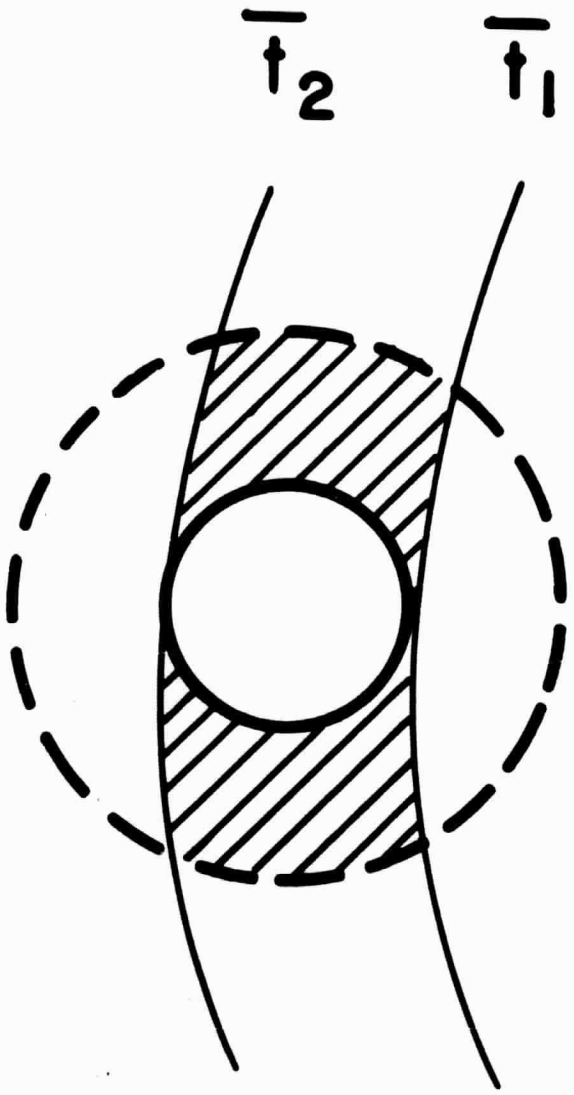

Fig. 6

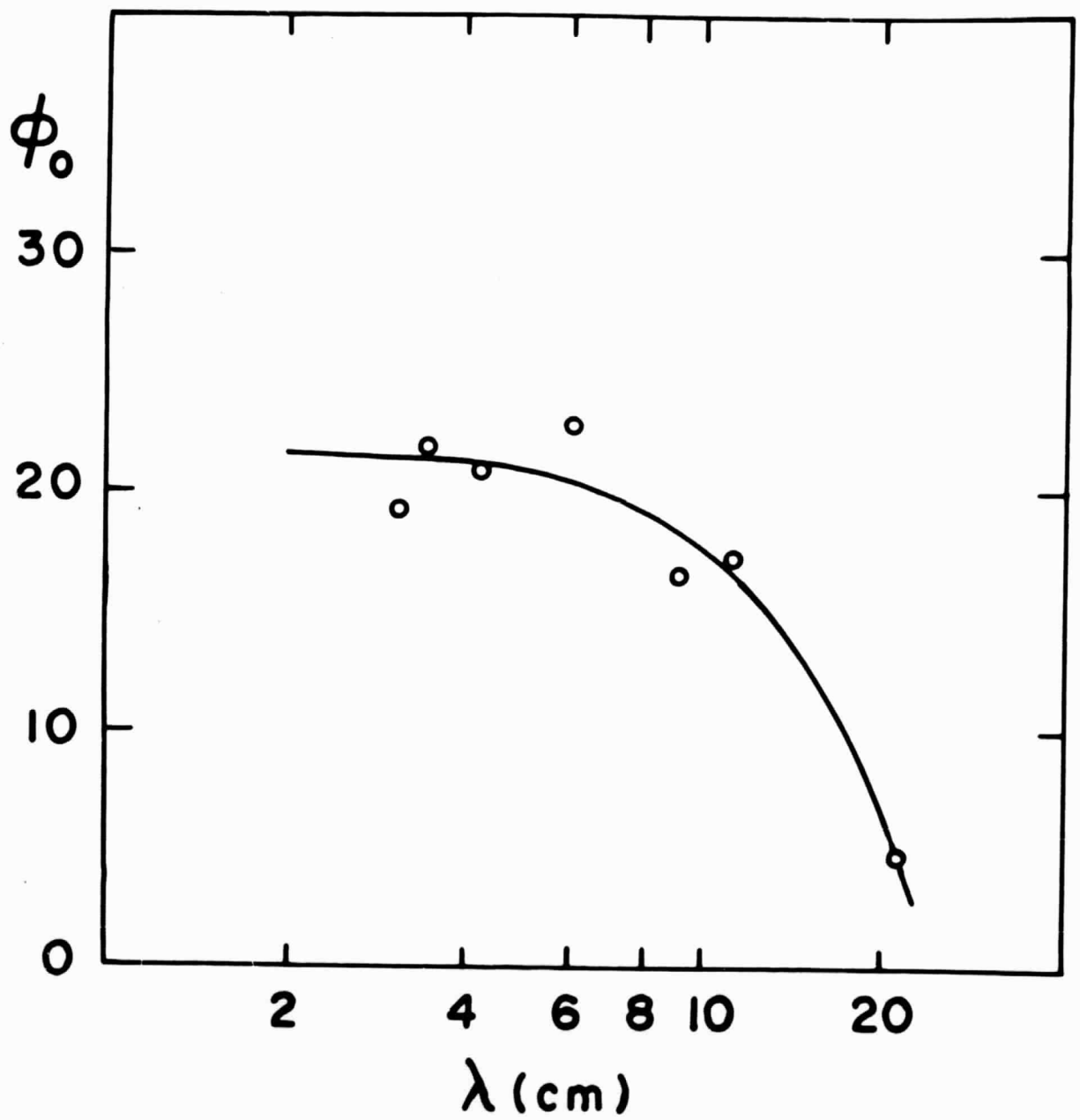

Fig. 7

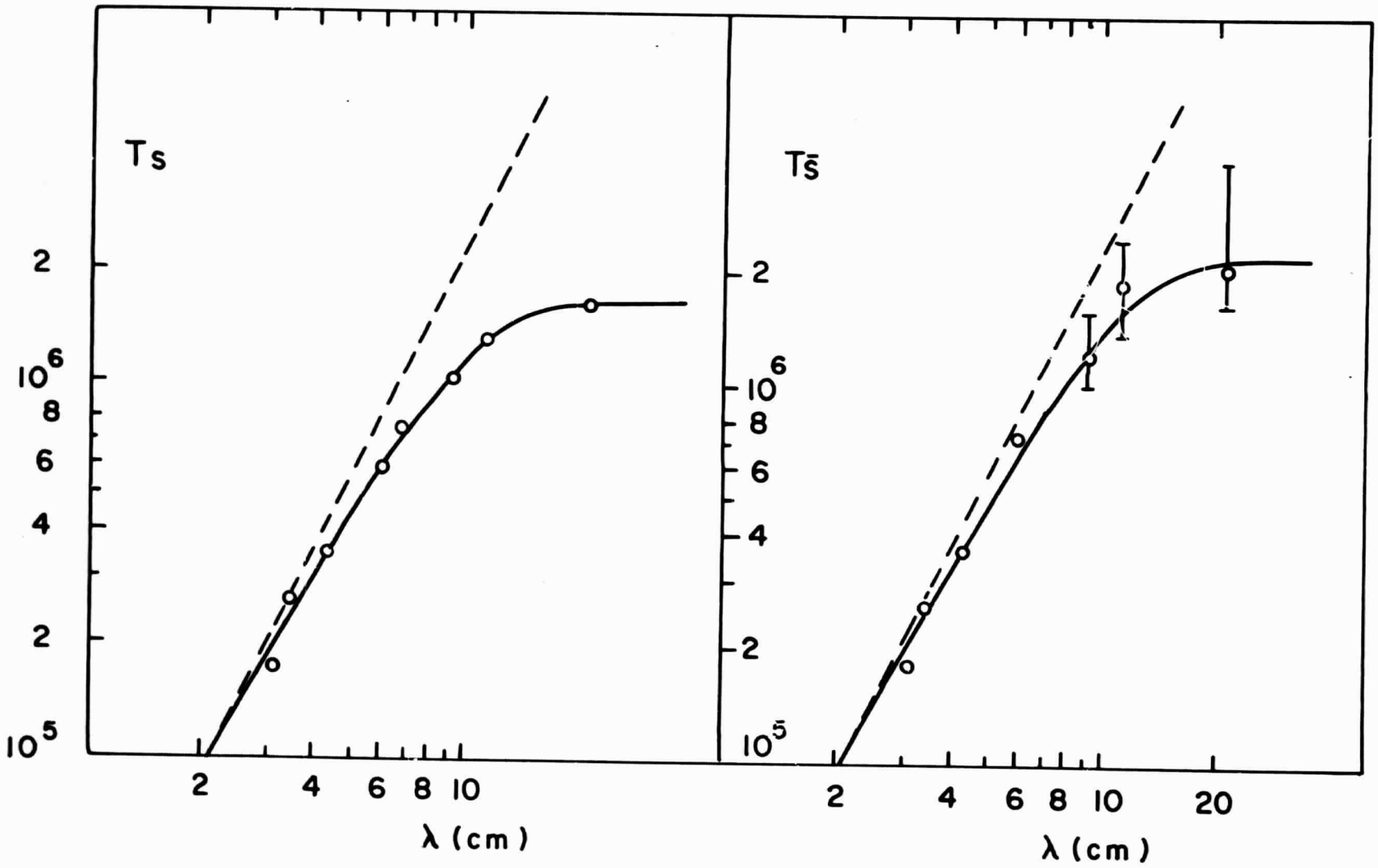

Fig. 8